Carbohydrate Polymers 93 (2013) 718–730

Contents lists available at SciVerse ScienceDirect

Carbohydrate Polymers

journal homepage: www.elsevier.com/locate/carbpol

# Multilayered textile coating based on a β-cyclodextrin polyelectrolyte for the controlled release of drugs

Adeline Martin[a], Nicolas Tabary[a], Laurent Leclercq[b], Jatupol Junthip[a], Stéphanie Degoutin[a], François Aubert-Viard[d], Frédéric Cazaux[a], Joël Lyskawa[a], Ludovic Janus[a], Marc Bria[c], Bernard Martel[a,*]

[a] Université Lille 1, Unité Matériaux et Transformations (UMET) UMR CNRS 8207, Villeneuve d'Ascq, France
[b] Université Montpellier 1, Institut des Biomolécules Max Mousseron (IBMM) UMR CNRS 5247, Montpellier, France
[c] Université Lille 1, Centre Commun de Mesures RMN, Villeneuve d'Ascq, France
[d] INSERM U 1008, Controlled Drug Delivery Systems and Biomaterials, Lille, France

ARTICLE INFO

*Article history:*
Received 8 September 2012
Received in revised form
14 December 2012
Accepted 19 December 2012
Available online 27 December 2012

*Keywords:*
Non-woven textile
Layer-by-layer
Drug release system
Chitosan
Cyclodextrin polymer
OWLS

ABSTRACT

The aim of this work was to develop the formation of multilayered coating incorporating a cyclodextrin polyelectrolyte onto a non-woven polyethylene terephthalate (PET) textile support in order to obtain reservoir and sustained release properties towards bioactive molecules. We optimized the multilayer assembly immobilization onto the PET surface according to the layer-by-layer (LbL) deposition process. After a pre-treatment of the textile support aiming to offer a sufficient ionic character to the surface, it was alternatively immersed into two polyelectrolytes aqueous solutions consisting of chitosan (CHT) as polycation on the one hand, and a β-cyclodextrin polymer (polyCTR-βCD) as polyanion on the other hand. In a second approach, a TBBA/polyCTR-βCD complex (4-tert-butylbenzoic acid, TBBA) was used in order to load the system with a drug model whose kinetics of release was assessed. Gravimetry, microscopy, OWLS, colorimetric titration, infrared and zetametry were used as characterization techniques. An effective deposition on the textile surface due to ionic interactions with alternation of up to 10 layers of each of both polyelectrolytes was clearly evidenced. However, we observed that layer formation occurred to a lesser extent when TBBA/polyCTR-βCD complex was applied instead of polyCTR-βCD alone. The release study showed that drug reservoir properties and release kinetics could be controlled by the number of layers in the system and that TBBA release was faster than the multilayered coating degradation.


## 1. Introduction

Biomaterials are currently used in a wide range of surgical specialties. Their function consists of replacing, reinforcing or repairing failing organs. Despite the chemical stability and biocompatibility of raw materials used in their manufacture, such implants frequently cause side effects such as inflammation, thrombosis, or infections and involve some short or long term post operatory complications that may prolong the healing period or provoke mortality in the worst cases (Franz, Rammelt, Scharnweber, & Simon, 2011). In the last two decades some efforts have been made by researchers to find solutions in order to improve the tissue integration of medical implants in the body (Elvin et al., 2010; Teo et al., 2011). Among the most efficient solutions, surface treatment of biomaterials has been investigated aiming to modify their physicochemical properties to control cell proliferation or adhesion (Gendron et al., 2012; Lawrence et al., 2012), or to reduce bacterial colonization (Niţescu, Dumitriu, Dumitru, Trăistaru, & Burlibaşa, 2012). Another strategy consisted of transforming the device into a drug delivery system capable of releasing some drugs or bioactive substances (Degoutin et al., 2012; García-González, Alnaief, & Smirnova, 2011). In this case, the main challenges are firstly to chemically modify such inert materials with soft methods in order to keep their original properties (biocompatibility, mechanical resistance), and secondly to adsorb a sufficient therapeutic dose of the drug that should then be released covering the critical healing period.

Cyclodextrins (CDs) and their polymers have proved to be appropriate candidates for this purpose (Uekama, Hirayama, & Irie, 1998). Due to the hydrophobic character of their cavities, they are known to form reversible inclusion complexes with many hydrophobic bio-active molecules and promote their solubility (Connors, 1997; Loftsson & Brewster, 1996). Therefore, CDs are widely used for their encapsulation properties as drug carriers (Li, Xiao, Li, & Zhong, 2004; Rajewski & Stella, 1996; Sun et al., 2012; Uekama et al., 1998).

* Corresponding author at: Université Lille 1, Unité Matériaux et Transformations, Bâtiment C6, Bureau 119, 59655 Villeneuve d'Ascq, France. Tel.: +33 3 20 43 46 35; fax: +33 320 43 65 91.
*E-mail address:* bernard.martel@univ-lille1.fr (B. Martel).

0144-8617/$ – see front matter © 2012 Elsevier Ltd. All rights reserved.
http://dx.doi.org/10.1016/j.carbpol.2012.12.055

Owing to an original pathway to fix cyclodextrins onto porous and fibrous materials, our group has published many papers concerning biomaterials with improved reservoir and sustained delivery of antibiotics. For example, treated materials include hydroxyapatite porous ceramics as bone substitutes (Leprêtre et al., 2009; Tang, Zhao, Sha, & Liu, 2012), PVDF membranes applicable to guided tissue regeneration in periodontology (Boschin et al., 2006; Leprêtre et al., 2007; Tabary et al., 2007) and to a greater extent, vascular (Blanchemain et al., 2005, 2007a, 2007b, 2011) and parietal textile implants (El Ghoul et al., 2008; Laurent et al., 2011).

The present work aims to describe an evolution of the latter fixing concept by applying the layer-by-layer (LbL) approach. Over the past several years, Decher and others developed the layer-by-layer process (Decher, Hong, & Schmitt, 1992; Decher & Schmitt, 1992; Decher, 1997; Dubas & Schlenoff, 2001) as a tool for surface modification on various materials like quartz substrate (Decher et al., 1992; Decher & Schmitt, 1992), glass (Lvov, Decher, & Moehwald, 1993), cotton woven fabric (Karimpil, Melo, & D'Souza, 2012; Wang & Hauser, 2009) or cellulose (Deng et al., 2010). Among the possible techniques of polyelectrolytes multilayer build-up (Seantier & Deratani, 2012), dip-coating consists of dipping samples alternatively in anionic and cationic polyelectrolyte solutions, allowing adsorption by electrostatic interactions and then formation of multilayer assemblies over the substrate. This technique is fast, easy to use, with a soft and biocompatible process (mainly in water) and seems to be adjustable to any kind of substrates.

The application of the LbL technique for biological or biomedical purposes requires the use of bioactive polyelectrolytes in the build up, or by loading a low molecular bioactive compound in the multilayer assembly (Burke & Barrett, 2003; Caruso, Niikura, Furlong, & Okahata, 1997; Lvov, Ariga, Ichinose, & Kunitake, 1995). For instance, literature abundantly reports the use of chitosan as positive polyelectrolyte incorporated in the LbL coating, which offers its intrinsic antimicrobial properties to treated surfaces (Fu, Ji, Yuan, & Shen, 2005) throughout extended degradation of the assembly.

Using LbL assembly for its reservoir properties towards drugs was previously reported (Benkirane-Jessel et al., 2004; Gribova, Auzely-Velty, & Picart, 2011). This path requires complexation or hosting properties of the cationic and/or anionic polyelectrolytes towards the targetted active molecule. In this case the use of cyclodextrin, well known for its host–guest complexation properties, is one of the most relevant solution. For example, encapsulated piroxicam in cyclodextrins was used to build a multilayer assembly with anti-inflammatory properties (Benkirane-Jessel et al., 2004). Biological activity was still present after 12 h, even if the maximum activity was found after few hours.

Our strategy was based on both of the above mentioned approaches, wherein chitosan was used as the cationic polyelectrolyte. This natural and biocompatible polymer is often used in biomaterials (Costa-Júnior, Barbosa-Stancioli, Mansur, Vasconcelos, & Mansur, 2009; Rinaudo, 2006; Venkatesan, Ryu, Sudha, & Kim, 2012) due to its well-known intrinsic antibacterial and hemocompatible properties (Bhardwaj & Kundu, 2011) and its ability to be incorporated in multilayer assemblies on solid surfaces (Lin, Ren, & Ji, 2009; Fu et al., 2005). Its role is to ensure insertion of the anionic cyclodextrin polymer in the multilayer system, and also to ensure its relative stability, as a result of its slow biodegradation. The polyanionic specie polyCTR-βCD is a water soluble cyclodextrin polymer issued from the crosslinking reaction between citric acid (CTR) and βCD (Martel, Morcellet, Ruffin, Ducoroy, & Weltrowski, 2002; Martel, Morcellet, & Weltrowski, 2002; Martel, Weltrowski, Ruffin, & Morcellet, 2002; Martel, Ruffin, Weltrowski, Lekchiri, & Morcellet, 2005) known for its ability to complex drugs (Bakkour et al., 2006; Joudieh, Bon, Martel, Skiba, & Lahiani-Skiba, 2009). So far, multilayer systems including cyclodextrins based polyelectrolytes for drug delivery purposes have never been reported. Dubacheva studied neutral polymers, where layers interfered by host–guest complexation between hydrophilic polymers bearing cyclodextrins as pendent groups on the one hand, and ferrocene groups on the other hand (Dubacheva et al., 2010). Semenov et al., reported the gelation of associating polymer systems, where polymeric hyaluronan-based or chitosan-based backbones were modified with cyclodextrin and adamantane as associating groups (Semenov, Charlot, Auzély-Velty, & Rinaudo, 2007). Though, in such systems the cyclodextrin's role was to ensure the association with the other polymeric species, but not to deliver any drug.

Because of its low cost, chemical stability, mechanical properties and biocompatibility, PET is a widespread biomaterial (Chen & McCarthy, 1997; Köstler, Ribitsch, Stana-Kleinschek, Jakopic, & Strnad, 2005) especially used for vascular implants, inguinal meshes or sutures (Franklin et al., 2009). For these reasons a non-woven PET substrate was chosen in the present study. In order to ensure the adhesion of the multilayer coating onto the textile, a pretreatment is required to impart charge density onto the fibre surface. Therefore, we applied a previously described method that transformed raw PET into an ion exchange textile through a pad-dry-cure process, the resulting support bears carboxylate functions that would interact with the protonated amino groups of the first chitosan layer of the LbL system (Ducoroy, Bacquet, Martel, & Morcellet, 2007; Ducoroy, Martel, Bacquet, & Morcellet, 2007; Ducoroy, Bacquet, Martel, & Morcellet, 2008).

In this study we report the pretreatment of a PET textile support through the pad-dry-cure process, after which we describe the building of a self-assembled LbL coating monitored by optical waveguide lightmode spectroscopy (OWLS) (Abdelkebir et al., 2011; Lavalle et al., 2002; Ngankam, Mao, & Van Tassel, 2004; Ngankam & Van Tassel, 2005; Wittmer, Phelps, Saltzman, & Van Tassel, 2007). Then the LbL deposition was applied to the textile support by the dip-coating method, and followed by the weight gain of the samples versus the number of deposited layers. A characterization by zeta potential was assessed in the course of the successive depositions of polyCTR-βCD and chitosan layers. Acid orange titration allowed us to quantify chitosan deposition on supports versus the number of layers in the system. Once the drug model free system was characterized, LbL process was applied using the 4-*tert*-butylbenzoic acid (TBBA)/polyCTR-βCD complex. TBBA was selected for its known capability to form a stable inclusion complex with βCD (Auzély-Velty & Rinaudo, 2001; Weickenmeier, Wenz, & Huff, 1997; Wenz et al., 2008) and for its easy detection and titration by UV spectrophotometry in the bulk batch release medium. The targeted application of our new system will consist of the release of antimicrobial agents and in a second antiproliferative drugs in cancer therapies (Jang, Akgun, Kim, Satija, & Char, 2012).

## 2. Experimental

### 2.1. Materials

Non-woven polyethylene terephthalate (PET, weight = 65 g/m$^2$, thickness = 0.24 mm, reference NSN 365) was provided by PGI-Nordlys (Bailleul, France).

All commercial products were used as received. The native βCD used in this work was provided by Roquette (Lestrem, France). Citric acid (CTR), sodium hypophosphite monohydrate ($NaH_2PO_2{\cdot}H_2O$), sodium carbonate ($Na_2CO_3$), sodium hydroxide (NaOH), calcium acetate and 4-*tert*-butyl benzoic acid (TBBA) were commercial chemical grade products, supplied from Aldrich Chemicals

(St. Quentin Fallavier, France). Glacial acetic acid (99–100%) was a J.T. Baker product.

Chitosan low molecular weight grade ($59{,}200 < Mv < 65{,}000\ g\ mol^{-1}$, determined by viscosimetry) was purchased from Aldrich Chemicals. The 85% deacetylation degree of chitosan was determined by UV spectrophotometry using *N*-acetylglucosamine as reference in hydrochloric acid (Pedroni, Gschaider, & Schulz, 2003). This corresponded to 5 mmol of cationic ammonium functions per gram of chitosan.

### 2.2. Methods

#### 2.2.1. Pre-treatment of the textile support by pad-dry-cure

Textile samples were systematically thoroughly washed in soxhlet extractor with isopropanol, then with water (2 h and 3.5 h respectively) and dried during 30 min at 90 °C.

In order to allow ionic interactions between support and the first chitosan layer of the LbL assembly, we applied a pad-dry-cure textile finishing process previously reported (Ducoroy, Bacquet et al., 2007; Ducoroy, Martel et al., 2007; Martel, Morcellet, Ruffin et al., 2002; Martel, Morcellet, & Weltrowski, 2002; Martel, Weltrowski et al., 2002). The non-woven PET fabrics (10 cm × 5 cm) were impregnated by an aqueous solution containing βCDs, catalyst and CTR, whose composition is reported as 10/3/10 related to the weight in gram unit of βCDs, catalyst and CTR, respectively, dissolved in 100 mL of water. The textile was then roll-squeezed (Roaches, England) and dried at 90 °C for 5 min. Curing occurred in a thermo-fixation oven (Minithermo®, Roaches, UK) at 150 °C for 30 min. Finally, samples were thoroughly washed in soxhlet extractor (500 mL) with water during 3.5 h in order to remove unreacted products. The weight gain (WG) (%) representing the yield of the thermofixation reaction was calculated using the equation:

$$WG(\%) = \frac{(M_f - M_i) \times 100}{M_i}$$

where $M_i$ and $M_f$ correspond respectively to the sample weight before and after treatment, measured with a precision balance ($\pm 4.10^{-4}$ g). Before weighing, all samples were dried at 90 °C for 30 min. Experiments were performed in triplicate and averaged.

The above mentioned process resulted in the functionalization of the PET textile by a highly cross-linked polymer formed between βCD and CTR. This occurred via a polyesterification reaction between the latter reactants, forming a coating physically anchored onto the PET fibres (Fig. 1b) (Martel, Morcellet, Ruffin et al., 2002; Martel, Morcellet, & Weltrowski, 2002; Martel, Weltrowski et al., 2002).

The ion exchange capacity (IEC) of the thermofixed samples was determined using the calcium acetate method described in the United States Pharmacopoeia (USP 1995). 500 mg of textile sample were placed in 50 mL of a calcium acetate solution (2 wt%) for 1 h under magnetic stirring. The solution was filtrated and then titrated by a standard 0.05 N NaOH solution using phenolphthalein as indicator.

The amount of carboxylic functions was calculated by the following equation:

$$\mathrm{IEC\,(mmol/g)} = \frac{C_b \times V_e\,(\mathrm{mL})}{\mathrm{sample\ weight\,(mg)}}$$

where $C_b$ and $V_e$ correspond respectively to the concentration of the NaOH solution and the equivalent volume.

In this work, the thermofixed layer applied in the pre-treatment step was conventionally counted as layer 1.

#### 2.2.2. Water-soluble polyCTR-βCD synthesis

Water soluble polyCTR-βCD (structure in Fig. 1a) that was used as anionic polyelectrolyte in the LbL system was synthetized according to a method previously reported (Martel, Morcellet, Ruffin et al., 2002; Martel, Morcellet, & Weltrowski, 2002; Martel, Weltrowski et al., 2002; Martel et al., 2005).

Acid–base titration displayed the presence of 5 mmol of COOH functions per gram of polyCTR-βCD (Martel et al., 2005). Mw measured by size exclusion chromatography (SEC) in water equipped with a light scattering detector was $75{,}000\ g\ mol^{-1}$.

The structure corresponds to a crosslinked polymer network where each βCD moiety was linked to neighbouring βCDs by the intermediate of citrate crosslinks (see Fig. 1). The solubility in water of polyCTR-βCD was 1000 g/L, compared to the solubility of the native βCD (18.5 g/L).

#### 2.2.3. Layer by layer (LbL) construction

The multilayer assembly was built using the LbL method as reported by Decher et al. (1992) and Decher and Schmitt (1992). Samples (3 cm × 3 cm) were cut off from the previously cyclodextrin thermofixed textile as described above (cf. Section 2.2.1). In order to transform all surfacic carboxylic groups into carboxylate groups, all samples were dipped into a sodium carbonate $Na_2CO_3$ solution (0.1 M) for 10 min then rinsed three times with distilled water and dried for 30 min at 90 °C.

Successive adsorption and rinsing steps of the dip-coating technique were carried out at room temperature under stirring (150 rpm) as schematized in Fig. 2. Firstly, the thermofixed samples were dipped into 50 mL of a chitosan solution (5 g/L) solubilized in acetic acid 10 mL/L for 15 min (solution 1), dried at 90 °C for 15 min, rinsed with a 3 mL/L acetic acid solution for 15 min to remove excess of chitosan (solution 2) and finally dried at 90 °C for 15 min. Then the sample was dipped into a polyCTR-βCD aqueous solution (4 g/L) for 15 min (solution 3), dried at 90 °C for 15 min, rinsed with distilled water for 15 min (solution 4) and dried at 90 °C for 15 min. The next layers were deposited by applying this sequence *n* times. The first chitosan layer adsorbed onto the thermofixed layer was labelled as layer 2, while the following polyCTR-βCD layer was labelled layer 3, so self-assembled chitosan and polyCTR-βCD layers presented even and odd labels, respectively.

Same process was used to build multilayer assembly incorporating a model molecule. In this case, the anionic layer was formed by dipping the sample into an aqueous solution of polyCTR-βCD/TBBA complex. TBBA complexes with β-cyclodextrin have already been studied (Auzély-Velty & Rinaudo, 2001; Wenz et al., 2008) and show a stable 1:1 complex in solution whose formation constant value was $18{,}400\ mol^{-1}$ (Weisser, Nelles, Wenz, & Mittler-Neher, 1997). We confirmed this result by isothermal titration calorimetry (ITC), measuring a $17{,}000 \pm 1000\ mol^{-1}$ constant (with $n = 0.98$).

Because of the low solubility of TBBA in water (50 mg/L at 20 °C, pH = 4.3), the complex formed in multilayer assemblies is not stoichiometric. A saturated aqueous solution of TBBA was first prepared (50 mg/L). An excess of polyCTR-βCD (4 g/L) was then dissolved in the TBBA solution and left under stirring during 24 h. The molar ratio of TBBA to βCD units in polyCTR-βCD was 1:6. To obtain the TBBA complex incorporation in the multilayer system, the textile samples were dipped for 30 min in this solution, followed by a drying step at 90 °C for 15 min, rinsing with distilled water for 15 min and drying at 90 °C for 15 min.

The weight gain after each step was determined following this equation:

$$\mathrm{WG\,(\%)} = \frac{(M_n - M_i) \times 100}{M_i}$$

where $M_i$ and $M_n$ are respectively the weight of the starting raw PET and after the thermofixation step or after the deposition of the adsorbed layers by dip coating.

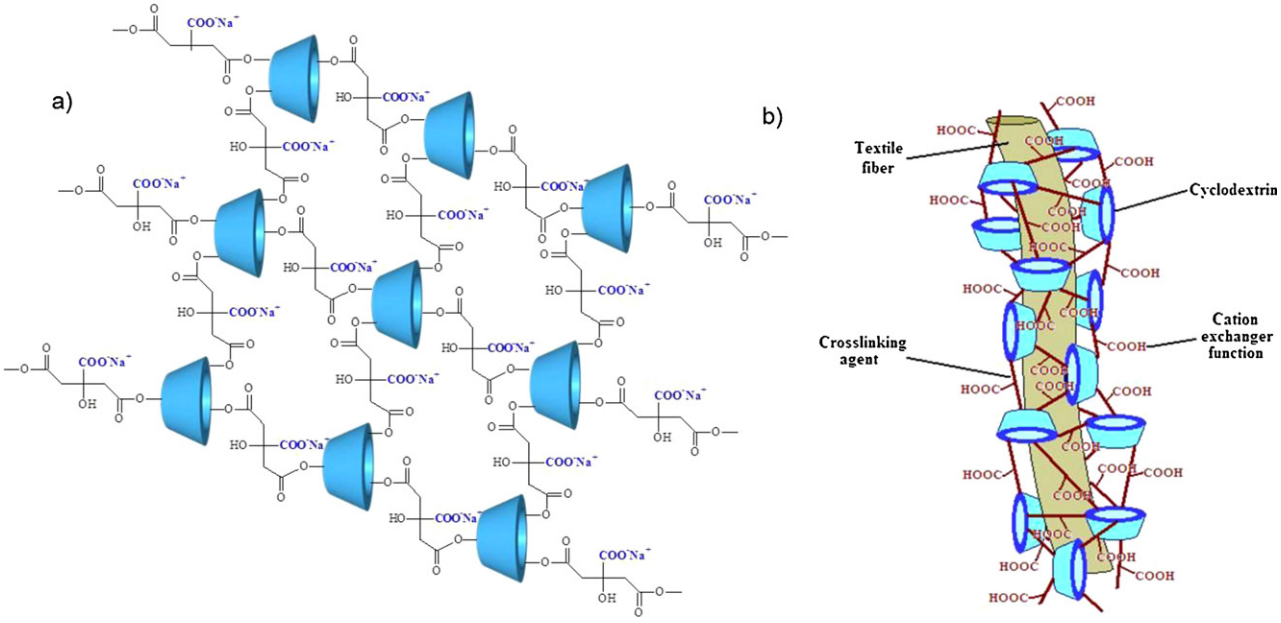


**Fig. 1.** (a) Schematic representation of the structure of the water-soluble polyCTR-βCD in its basic form, when synthetized in a reactor to yield polyCTR-βCD and (b) the same polymer, coating the PET fibres during the pad-dry-cure process (Ducoroy, Martel et al., 2007).

*2.2.4. Microscopy*

Samples were observed with an Olympus BX41 optical microscope. Scanning electron microscopy (SEM) investigations were carried out on a Hitachi S-4700 SEM FEG (Field Emission Gun) operating with an acceleration voltage of 5 KV. As the samples were non-conducting, they were covered with a conducting carbon layer to prevent charging.

*2.2.5. TGA*

Thermogravimetric analysis experiments were performed with a TGA Q50 apparatus (TA Instruments) from ambient to 500 °C with a heating rate of 5 °C/min. The sample was placed in an open platinum high temperature pan and the oven was flushed with highly pure nitrogen gas (90 mL/min).

*2.2.6. FTIR*

A PerkinElmer spectrometer (spectrum 1) equipped with Spectrum software was used to perform the FTIR analyses. The attenuated total reflectance (ATR) FTIR spectra (3 bounces) were collected from 16 scans in the 400–4000 $cm^{-1}$ range with a resolution of 4 $cm^{-1}$. Spectra of chitosan and polyCTR-βCD powders were performed from KBr pellets (1%w/w in KBr).

*2.2.7. Study of layer by layer adsorption by OWLS*

Optical waveguide lightmode spectroscopy (OWLS) is emerging as a powerful tool to investigate interactions of molecules and macromolecules on surfaces quantitatively (Gray, 2004; Scott et al., 2008; Tie, Calonder, & Van Tassel, 2003), including adsorption, binding and adhesion processes (Brusatori & Van Tassel, 2003; Eggleston et al., 2008; Kurrat, Textor, Ramsden, Boni, & Spencer, 1997; Kurrat, Prenosil, & Ramsden, 1997). The fundamentals of OWLS have been described in details (Tiefenthaler & Lukosz, 1989). In summary, a linearly polarized light (He–Ne laser) is coupled with the evanescent light by a diffraction grating into a waveguide layer, provided that the in-coupling condition is fulfilled. The in-coupling is a resonance phenomenon that occurs at two well-defined angles of incidence (electric and magnetic modes) depending on refractive index of the medium closely covering the surface of the waveguide. The light is guided by total internal reflection to the edges of the waveguide where it is detected by a photodiode. The sensor chip is based on a fine optical grating prepared on a thin waveguide layer carried by a glass substrate. Refractive index and thickness of the adsorbed molecules and hence adsorbed mass per unit area can be evaluated (Picart et al., 2001; Vörös et al., 2002). Like SPR, OWLS is label-free and its sensitivity is c.a. 1 $ng/cm^2$. Coating amount

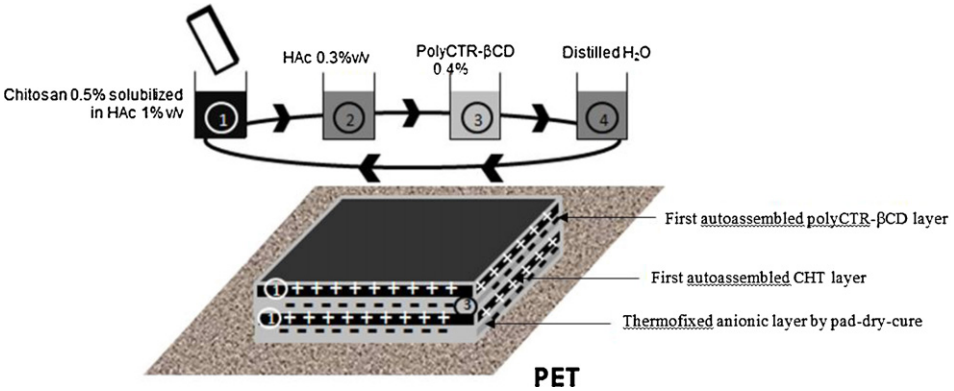


**Fig. 2.** Schematization of the layer-by-layer construction of the multilayer assembly by the dip-coating method applied on the pre-treated non-woven PET by pad-dry-cure. The thermofixed layer applied in the pre-treatment step was conventionally counted as layer 1.

and thickness were assessed using a Microvacuum Ltd. (Budapest, Hungary) OWLS 120 apparatus composed of a SIS06 standard subunit for sample injection, a controlled NE-1000 syringe pump and a 100 μL loop. The light source was a linearly polarized He–Ne laser emitting at 632.8 nm. The sample holder was kept at controlled temperature by a Peltier temperature control device governed by an Omron controller built into the TC unit. All the measurements and calculations were performed using the Biosense 2.6 software.

The sensor chip of the optical waveguide was based on a fine optical grating engraved on a thin waveguide layer carried by a glass substrate. The grating was 12 mm long and 2 mm wide, with a periodicity of 2400 lines/mm. Waveguide material was $Si_xTi_{(1-x)}O_2$, where $x = 0.25 \pm 0.05$ with a thickness (dF) of 165 nm. As the chip surface is negatively charged, the first polyelectrolyte to be injected is a polycation.

Prior to each experiment, the chip surface was cleaned by contact with a 4N $HCl/H_2SO_4$ aqueous solution and sonicated for 15 min prior to rinsing with water and acetone successively. The polyelectrolytes were injected at a concentration of 5 g/L for chitosan (in 10 mL/L acetic acid) and 6 g/L for the polyCTR-βCD (in 0.1 M phosphate buffer). Experiments were conducted under continuous 50 $mm^3$/min flow until a plateau was reached or at least well engaged when levelling off required too much time. Rinsing with 0.1 M phosphate buffer (pH = 4.8) was performed between each layer deposition to remove weakly adsorbed molecules that did not resist washing conditions. A maximum of 13 layers was applied. In OWLS experiments, intermediate rinsing conditions did not exactly correspond to those applied on textile and described in Section 2.2.3, because OWLS procedure needs the same buffer for baseline and washing solutions to suppress differences in refractive index.

Experiments were realized in triplicate and the standard deviation was about 10%.

#### 2.2.8. Zetametry

Zeta Potential was determined with a Zetacad apparatus at Ecole Nationale Supérieure des Arts et Industries Textiles (ENSAIT), Roubaix, France.

All samples were immersed during 24 h into a KCl aqueous solution ($10^{-3}$ M) and the pH was adjusted to the desired value using aqueous solutions of HCl and KOH (0.1 M). Measurements were realized in tetraplicate and averaged.

#### 2.2.9. Colorimetric titration with acid orange (AO)

Colorimetric titration with AO was used to determine quantity of amines issued from chitosan present on the surface (Hamerli, Weigel, Groth, & Paul, 2003; Uchida,Uyama, & Ikada, 1193).

A $2.5 \times 10^{-2}$ mol/L acid orange solution was prepared in distilled water and pH was adjusted to 3 using HCl 0.5 M. Each sample was dipped in 10 mL of this solution under stirring (60 rpm) overnight at 25 °C in order to adsorb AO. Samples were then washed twice for 5 min under stirring in 20 mL of acidic water (pH = 3, adjusted with 0.5 M HCl). Desorption occurred by immersing the samples into 10 mL of a solution at pH = 12 (adjusted with 0.5 M NaOH) for 24 h at 25 °C under stirring. Finally pH of each solution was adjusted to 3 with 1 mL of HCl 0.1 M and absorbance was measured at 485 nm.

A calibration curve was preliminarily made using the experimental procedure mentioned above on textile samples impregnated with a precise volume of a 10 g/L chitosan solution dissolved in acetic acid solution (10 mL/L) of and dried.

#### 2.2.10. Degradation of the multilayer assembly

Samples modified by the LbL process were placed in individual flasks in 50 mL of distilled water under stirring (100 rpm) on an orbital shaker thermostated at 37 °C (Thermoshake, Gerhardt, Les Essarts-le-Roi, France), periodically removed from the system, dried (30 min, 90 °C) and weighed; then put back in the flasks filled with 50 mL of fresh water. Reported data are the average values of 6 replicates. To evaluate the weight loss and to simultaneously compare assembly and degradation of the multilayers, the weight loss (WL in %) was calculated from the mass of the virgin PET as reference, following the equation:

$$\mathrm{WL}(\%) = \frac{(M_f - M_i) \times 100}{M_i}$$

where $M_i$ is the mass of the virgin PET without any treatment and $M_f$ is the mass of the treated support after the degradation at different times.

#### 2.2.11. TBBA release study

Textile samples (3 cm × 3 cm) were dipped in flasks containing 20 mL of distilled water under stirring (120 rpm) at 37 °C. To assess at the same time both the weight loss of the samples due to LbL system degradation and TBBA release in solution, samples were periodically removed from the batch, dried and weighed. At the same time, aliquots (2 mL) of the soaking solution were transferred into quartz cells (1 cm). The TBBA released in the bulk solution was determined by UV–vis spectroscophotometry (Shimadzu UV – 1800 Spectrometer) at 240 nm after calibration (molar extinction coefficient of TBBA in water was 0.0702 L $mg^{-1}$). Withdrawn aliquots were then returned into the batch solutions in order to keep the volume of the supernatant unchanged.

#### 2.2.12. Complexation study by NMR

All experiments were recorded using a spectrometer Brüker Avance™ 400 equipped with a Brüker Ultra-Shield 9.4 T (proton Larmor frequency of 400.33 MHz). We used a BBI probe ($^1$H, X). Two-dimensional NOESY experiments were acquired in the phase-sensitive mode using the Brüker ASX 400 (9.4 T) spectrometer. The probe temperature was regulated to 300 K. Each spectrum consisted of a matrix of 2 K (F2) by 2 K (F1) covering a sweep width of 4084 Hz. We used spin-lock mixing periods of 500 ms. Before Fourier transformation, the sine apodization functions were applied in both dimensions. 256 increments were collected with 80 transients in each.

## 3. Results and discussion

### 3.1. Pre-treatment of PET by thermofixation

Our strategy to promote the fixation of the LbL assembly onto the fibrous support consisted of the raw PET surface functionalization with a coating polymer rich in carboxylate groups that would promote the adsorption of the first chitosan layer. Therefore, we applied the process that was previously reported (Ducoroy, Bacquet et al., 2007; Ducoroy, Martel et al., 2007) and yielded ion exchange properties to the textile. In the present case, Fig. 3 shows the parallel evolution of the weight gain and IEC of the support with time and curing temperature. The weight gain is attributed to the coating of the fibres by the in situ crosslinking reaction between cyclodextrin and citric acid (Martel, Morcellet, Ruffin et al., 2002; Martel, Morcellet, & Weltrowski, 2002; Martel, Weltrowski et al., 2002).

Besides, IEC was reported as the amount in mmol of carboxylate groups per gram of support available on this thermofixed coating. As a matter of fact, increasing the density of negative electrostatic charges on the support surface should promote the interactions with the first cationic layer (chitosan), and with the whole multilayered coating.

As shown in Fig. 3, both weight gain and IEC presented a high limit value after 30 min of curing at 150 °C: 20 wt% and 0.7 mmol/g of textile, respectively. Besides, as curing time was set to 30 min and temperature was increased, IEC levelled off above 150 °C while the

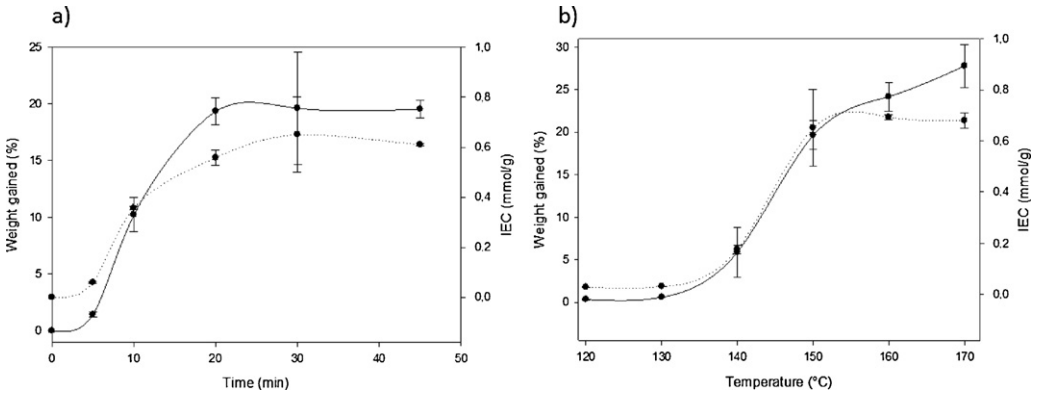


**Fig. 3.** Influence of the curing parameters on the weight gain (—) and ion exchange capacity (IEC) (···) of the pre-treated non-woven PET; (a) with time, temperature fixed at 150 °C; (b) with temperature, curing time fixed at 30 min.

weight gain of the sample still increased. This feature was noticed in a previous study where we even reported a decrease rather than a stagnation of the IEC, that we attributed to a high conversion rate of the carboxylic groups of CTR residues into ester groups through the reaction with the polysaccharidic hydroxyls (Ducoroy, Bacquet et al., 2007; Ducoroy, Martel et al., 2007).

So, setting the curing parameters at 150 °C for 30 min yielded the highest carboxylate functions available for immobilizing the superior layers.

### 3.2. Building of the multilayer assembly

#### 3.2.1. Monitoring approach by OWLS

The build-up of the multilayer assembly was followed in situ by OWLS. Chitosan and polyCTR-βCD were alternatively deposited on a $SiO_2/TiO_2$ anionic waveguide surface. This was repeated in order to cumulate n layers on the surface, even and odd *n* values corresponding to chitosan, and polyCTR-βCD layer respectively.

For better comprehension of OWLS spectrum, evolution of mass and thickness on an assembly of 3 layers was shown in Fig. 4a. Sharp peaks corresponded to the injections of polyelectrolytes. As soon as a plateau was obtained, rinsing step was carried out to remove non-adsorbed components, leading to a decrease of the mass deposited and to a new plateau. As seen, there are no big differences between mass deposited of anionic or cationic layers.

Fig. 4b shows the OWLS signal with time on an assembly of 13 layers. Fig. 4c was plotted from the plateau values measured after each rinsing step, in function of the number of layers. The evolution of the thickness of the 13-layers system was also reported in nm, calculated from the layer data. After the three first layers, a regular

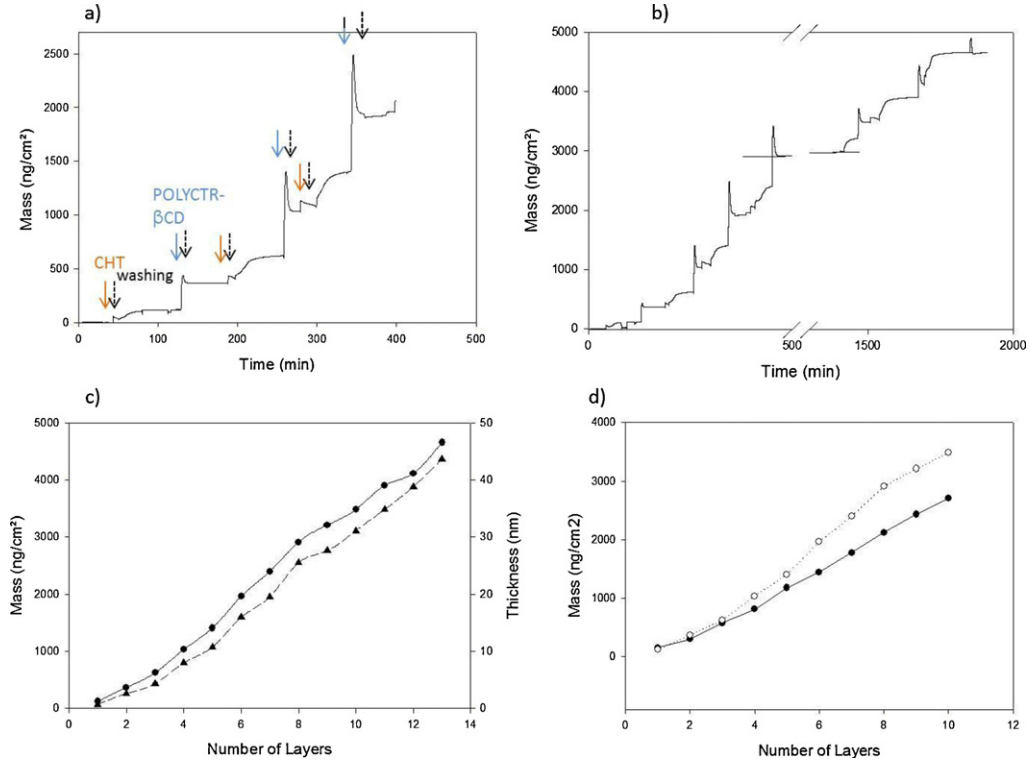


**Fig. 4.** (a) Evolution of the first 3 self-assembled layer film mass in ng/cm$^2$ followed by OWLS; ([chitosan] = 5 g/L in 10 mL/L HAc, [polyCTR-βCD] = 6 g/L in phosphate buffer solution pH = 4.8, washing between injections with phosphate buffer solution pH = 4.8); (b) evolution of the film mass of 13 layers in ng/cm$^2$ followed by OWLS; ([chitosan] = 5 g/L in 10 mL/L HAc, [polyCTR-βCD] = 5.2 g/L in phosphate buffer solution pH = 4.8, washing between injections with phosphate buffer solution pH = 4.8); (c) evolution of the cumulative mass (●) and thickness (▲) deposited on the surface against the number of deposited layers (13 layers); (d) evolution of cumulative mass deposited on the surface against the number of layers with (●) and without (○) encapsulated TBBA in the assembly.

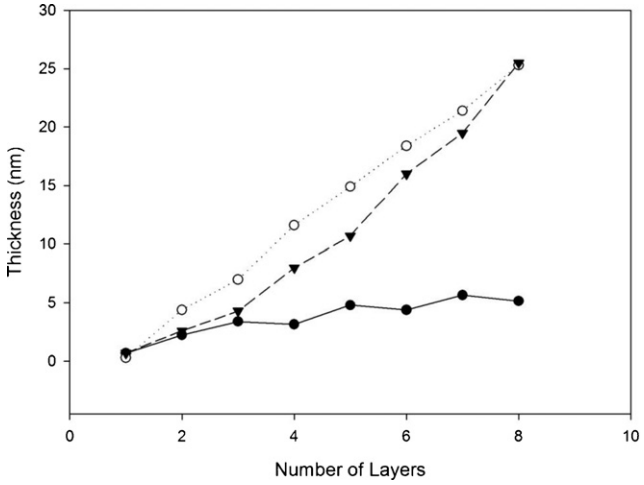


**Fig. 5.** Evolution of the film thickness obtained by LbL deposition of polyelectrolytes on the OWLS chip at different ionic strengths: NaCl 0 M (▼), NaCl 0.1 M (○), NaCl 1 M (●) ([chitosan] = 5 g/L in 10 mL/L HAc, [polyCTR-βCD] = 5.2 g/L in phosphate buffer solution pH = 4.8, washing between injections with phosphate buffer solution pH = 4.8).

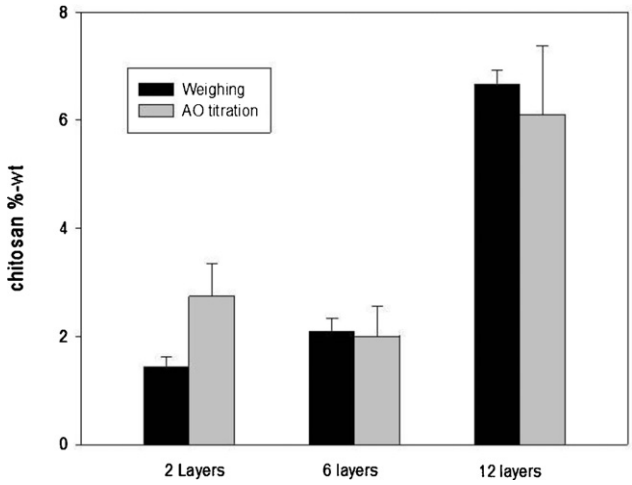


**Fig. 7.** Chitosan quantities determined by weight gain (black bars) and by acid orange titration (grey bars) with different numbers of layers at the surface.

evolution of the multilayer system was observed, with an average thickness of 2.85 nm/layer.

Fig. 5 reports ionic force influence on the build-up of the polyelectrolyte multilayer. As observed, a high ionic force (1 M) prevented building of the multilayer. The thickness obtained in 1 M NaCl was low (compared to that under lower saline conditions). Under high ionic strength conditions, it was found that the roughness on the surface increased (Lvov et al., 1993), which caused perturbations in the multilayer assembly. Moreover, it is well known that polyelectrolytes adsorb in a "flat" conformation in the absence of salt, whereas at higher ionic strength they adsorb in a "loop" conformation (Decher et al., 1992; Decher & Schmitt, 1992), and screen effects are stronger than electrostatic interactions. A very high ionic strength caused a desorption of previous layers due to a swelling effect (Dubas & Schlenoff, 2001). Fig. 5 shows that at low ionic strength or in the absence of salt, the building was optimal with thickness reaching 25 nm after the deposition of 6 layers.

OWLS indicated also that at low pH (pH < 2) it was not possible to adsorb polyCTR-βCD onto the first chitosan layer, so the carboxylate form of polyCTR-βCD should be required rather than the carboxylic form, which confirms the electrostatic interactions involved in the LbL process.

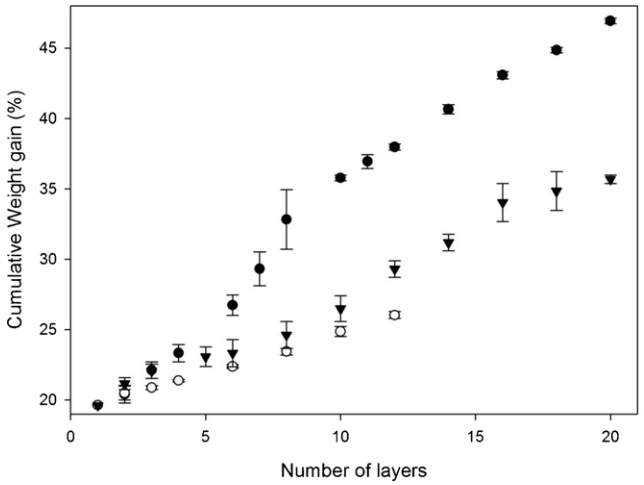


**Fig. 6.** Evolution of cumulative weight gain with the number of layers on PET support for the multilayer assembly at different concentrations: (●) chitosan = 5 g/L in 10 mL/L HAc and polyCTR-βCD = 4 g/L in $H_2O$, (○) chitosan = 2.5 g/L in 10 mL/L HAc and polyCTR-βCD = 2 g/L w/v in H2O, and (▼) chitosan = 5 g/L in 10 mL/L HAc and polyCTR-βCD = 4 g/L in a 50 mg/L aqueous solution of TBBA.

### 3.2.2. LbL build-up onto pre-treated textile samples

The textile supports pre-treated by thermofixation were preliminarily dipped in a sodium carbonate (0.1 M $Na_2CO_3$) solution in order to provide carboxylate groups onto their surface. Then, they underwent the LbL treatment with chitosan ($C$ = 5 g/L) and polyCTR-βCD, ($C$ = 4 g/L) in absence of any additional salt. The same experiment was applied in the presence of twice diluted solutions (chitosan ($C$ = 2.5 g/L) and polyCTR-βCD ($C$ = 2 g/L)). Fig. 6 shows the evolution of the weight gain of the samples treated in both conditions. One can observe that the initial weight gain after thermofixation was WG = 19.6%. For the 3 next layers, the measured weight gains were in the same range. However, from the fourth layer, it was observed that the growth of the multilayer system in concentrated conditions was approximately twice that in diluted conditions. The weight gain due to LbL assembly in the concentrated conditions after 12 layers deposition was WG = 18.4 wt%, while this value reached only WG = 6.4 wt% in the semi diluted system. After 20 layers, the total weight gain measured was WG = 47 wt%, including 27.4 wt% due to LbL assembly, and 19.6 wt% to the thermofixed polyCTR-βCD layer. Those values

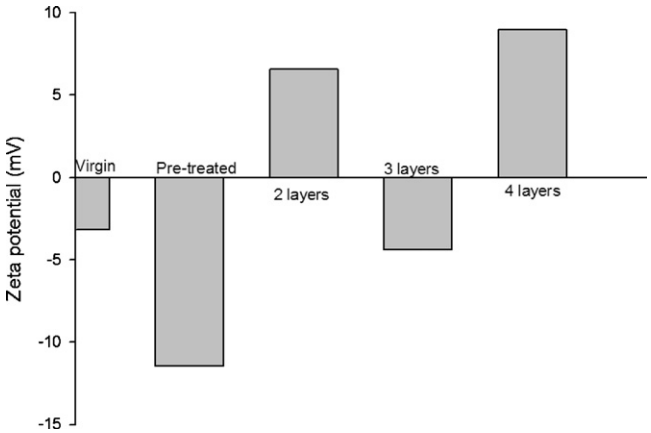


**Fig. 8.** Evolution of the zeta potential of samples with the number of layers (for 4 layers) deposited on the textile surface at pH = 4.

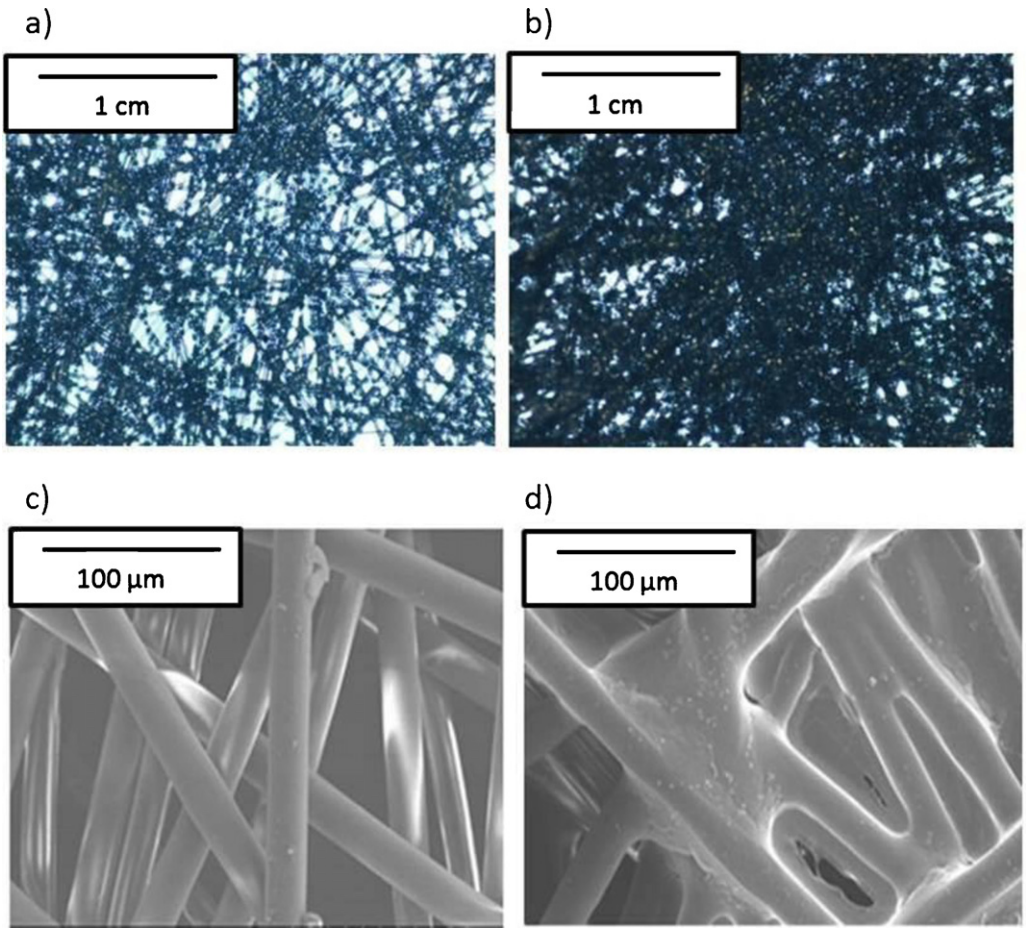


**Fig. 9.** Optical microscopy images (5×) of non-treated PET (a) and PET with 4 layers (b) and SEM images of non-treated PET 450× (c) and PET with 4 layers 400× (d).

correspond to an average weight increase of 1.4% per absorbed layer without any distinction between their cationic or anionic nature.

Fig. 7 shows the comparative study of the quantification of deposited chitosan by weight gain and acid orange titration after deposition of 3, 5 and 11 layers onto pre-treated support. Acid orange titration displayed increasing amounts of chitosan deposited with the number of layers (1.5%, 2.1%, and 6.7% respectively). The same behaviour was observed with gravimetric analysis, especially for the highest chitosan contents of the supports which confirms the formation of the multilayer assembly.

### 3.2.3. Zetametry

Fig. 8 shows evolution of the zeta potential of the textile surface over the first steps of its modification. The study was carried out at pH = 4 where both chitosan and polyCTR-βCD are in their ionic form (pKa $NH_3^+/NH_2$ = 6.2–7.32 for chitosan (Lee, Lim, Chong, & Shim, 2009), pKa $COOH/COO^-$ = 5.2–7.9 for polyCTR-βCD). At pH = 4, non-treated PET presented a negative zeta potential (−3 mV) in accordance with previous results (Smole et al., 2002), due to hydrophobicity of PET. After thermofixation, zeta potential decreased to −11 mV due to presence of carboxylate groups in the crosslinked polyCTR-βCD layer. A first reversal was observed after chitosan deposition (+6 mV) on the previous layer through electrostatic interactions. Then, a second reversal occurred upon the first self-assembled polyCTR-βCD layer (−4 mV) deposition. The difference of the extent of the zeta potential values between thermofixed and self-assembled layers are due to the difference between the carboxylate groups density brought through the thermofixation step on one hand, and those brought by ionic interactions in the LbL method on the other hand. As a matter of fact, the weight increase due to pre-treatment by thermofixation was in the range of 20 wt% while it was only 1.4 wt% in the case of the LbL process, as mentioned above. Finally, the second chitosan self-assembled layer presented again a positive zeta potential (+9 mV). These results confirmed the alternation of anionic and cationic layers on the textile surface upon the repeated cycles of the process.

### 3.2.4. Microscopy characterization

Images obtained from optical microscopy (Fig. 9a and b) clearly shows a reduction of the pore size of the textile structure upon

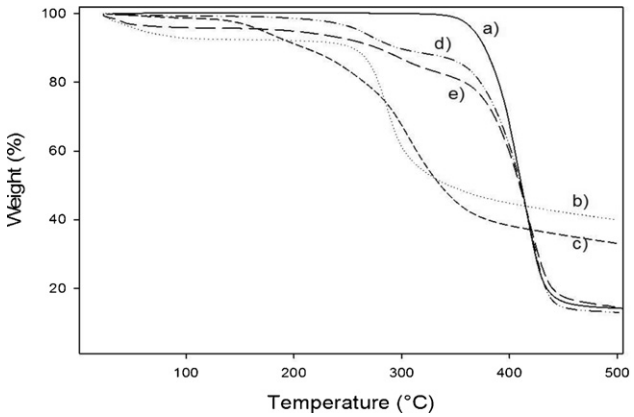


**Fig. 10.** TGA plots (5 °C/min, under nitrogen atmosphere) of virgin PET (a), chitosan (b), polyCTR-βCD (c), pre-treated PET by pad-dry-cure (150 °C – 30 min) (d), and pre-treated PET with 20 layers (e).

treatment. This functionalization was further demonstrated by SEM (Fig. 9c and d) where one can observe a significant polymer deposition onto the fibres with a partial filling of the gaps.

### 3.2.5. Thermogravimetric analysis

Fig. 10 shows the TGA curves (5 °C/min) of the virgin PET (a), chitosan powder (b), polyCTR-βCD powder (c), pre-treated PET by thermofixation (initial WG = 19.6 wt% determined by weighing) (d) and PET with 20 layers ($c_1$ = [chitosan] = 0.5% w/v, $c_2$ = [polyCTR-βCD] = 0.4% w/v, WG = 46.6 wt% determined by weighing) (e). Below 200 °C, the small loss of mass observed could be attributed to the polymers dehydration. Thermal degradation of untreated PET started at 350 °C, while that of chitosan and polyCTR-βCD started at 250 °C and 150 °C respectively. Due to the difference of the degradation temperature range between the raw support and the coating polymers, the degradation profiles of the pre-treated and 20 layers treated PET showed an evolution that clearly evidenced the functionalization of the textile by the polyelectrolytes through a weight loss appearing at 250 °C on the corresponding curves.

### 3.2.6. FTIR analysis

As observed in Fig. 11, infrared spectra of polyCTR-βCD and chitosan present both the characteristic bands of polysaccharides: elongation of hydroxyl, amino (CHT) and carboxylic (polyCTR-βCD) groups are revealed by the broad absorption bands at 3300 $cm^{-1}$. A combination of the elongation of COOH and ester (COOR) groups of polyCTR-βCD may be visualized at 1700 $cm^{-1}$ and finally at 1100 $cm^{-1}$ the anomeric and inter-glycosidic C—O—C links

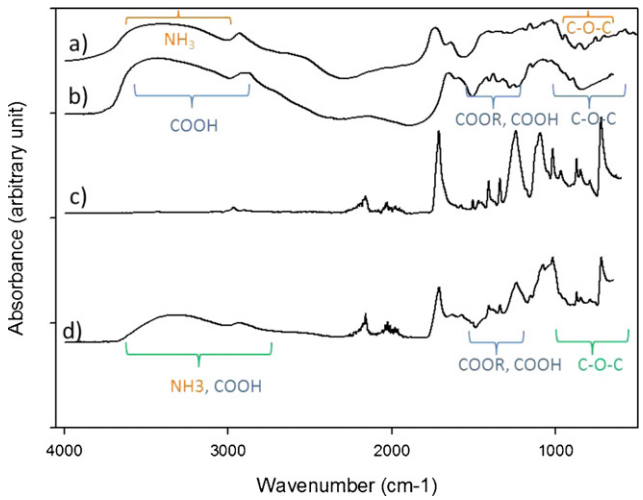


**Fig. 11.** FTIR spectra of chitosan powder from KBr pellets (a), polyCTR-βCD powder from KBr pellets (b), ATR spectra of virgin PET (c) and ATR spectra of PET with 20 layers (d).

elongation are also clearly visible on both spectra. Changes between non-treated PET and 20 layers PET display the presence of both polyelectrolytes on the support through the appearance of the large bands mentioned above, mixed to the characteristic bands of the polyethylene terephthalate support.

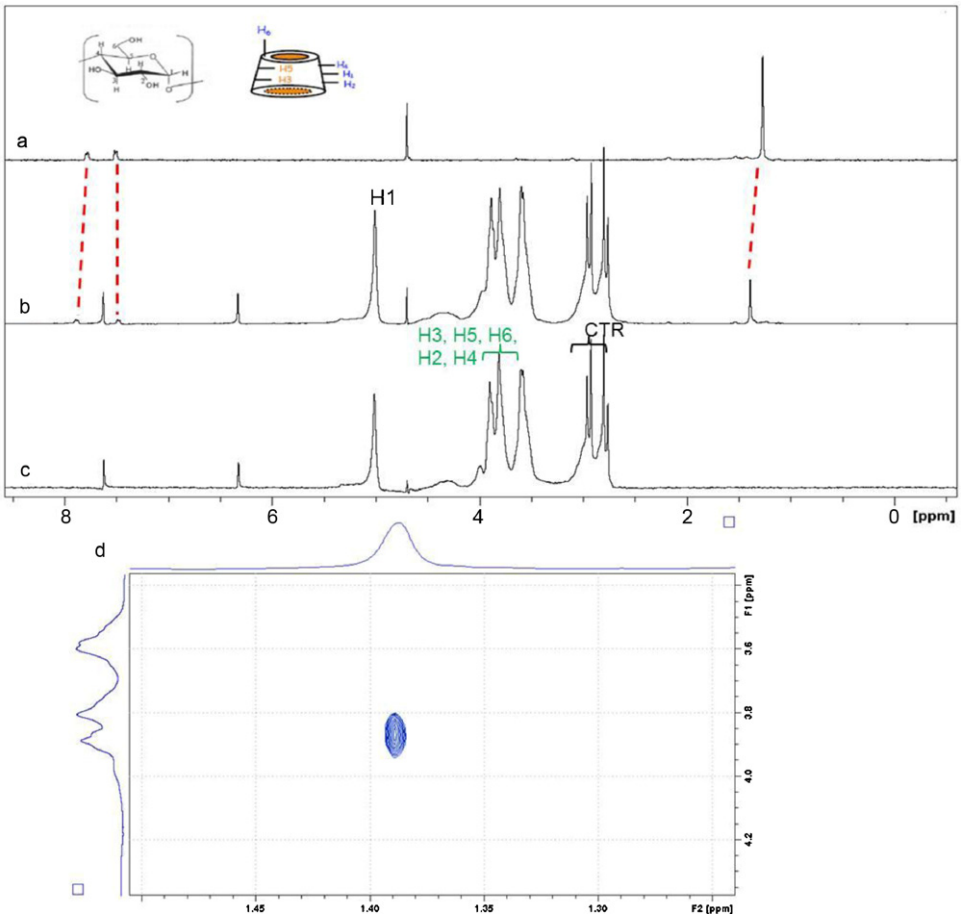


**Fig. 12.** (1) $^1H$ NMR in $D_2O$ of (a) TBBA; (b) TBBA-polyCTR-βCD complex and (c) polyCTR-βCD and (2) 2D-Noesy NMR spectrum focused on the cyclodextrin protons of polyCTR-βCD (vertical) and the tertiobutyl signal of TBBA (horizontal) in $D_2O$.

### 3.3. Building of the TBBA loaded multilayer system

#### 3.3.1. NMR study of the polyCTR-βCD/TBBA complex

A proton NMR study was developed in order to evidence the complexation between TBBA and polyCTR-βCD. Spectrum in Fig. 12a displays the NMR spectrum of TBBA where aromatic (doublets 7.45–7.52 and 7.77–7.79 ppm) and protons belonging to the tertiobutyl group (singlet 1.27 ppm) are observed. Besides, spectrum in Fig. 12c relative to polyCTR-βCD displayed the signal of the glucopyranosic units of cyclodextrins, H1 at 5.01 ppm, H3, H5, H6, H4 and H2 situated between 3.58 and 3.99 ppm, the methylene groups of the citrate crosslinks appearing between 2.76 and 2.96 ppm. Finally two singlets at 6.32 and 7.62 ppm corresponding to cis and trans aconitic esters, respectively. The latter species were issued from a side reaction consisting of the dehydration of citrate crosslinks (Wyrzykowski, Hebanowska, Nowak-Wiczk, Makowski, & Chmurzyński, 2011). Based on the integrations values of H1 (CD) and citrate methylene signals, we could calculate that one CD moiety was substituted in average by 5 citrate crosslinks. This also meant that the weight ratio of cyclodextrin moieties in polyCTR-βCD was close to 50% while the remaining part corresponded to the citrate crosslinks.

The spectrum in Fig. 12b is relative to the TBBA-polyCTR-βCD mixture, where the aromatic protons of TBBA shifted upfield and downfield to 7.47–7.49 and 7.87–7.89 ppm, and the tertiobutyl signal shifted downfield to 1.39 ppm. As observed in Fig. 12d, the 2D NOESY NMR Spectrum obtained from the NOESY sequence displays a correlation due to the dipolar interaction between the TBBA tertiobutyl group (1.39 ppm) and the H3 of βCD situated inside the cavity (3.86 ppm). Despite no evident interaction displayed between the aromatic part of TBBA and H3 or H5 protons of βCD (area not displayed in Fig. 12), this study clearly confirmed the inclusion complexation of TBBA in the cyclodextrin polymer.

#### 3.3.2. Multilayer build-up

The TBBA loaded multilayer system was built onto the pre-treated textile by alternative dippings in chitosan and polyCTR-βCD/TBBA complex solutions. Fig. 6 shows the evolution of the weight gain of the assembly, in comparison with the TBBA free system mentioned above. It is observed that the weight increase after each impregnation step in both solutions was sharply lowered in the presence of TBBA. As a matter of fact, results display that after thermofixation and 18 deposited layers, the total WG of the fabric was only 34.8 wt% in the presence of TBBA, against 44.8 wt% in TBBA free conditions. Considering that the contribution of pre-treatment corresponded to 19.6 wt%, the WG due to the self-assembled layers was 25.2% when free polyCTR-βCD was used, against 15.2% for the TBBA-polyCTR-βCD complex. In parallel, OWLS modelling results presented in Fig. 4d confirmed this tendency in a lesser extent than that observed on the textile support. These results showed that for constant polyelectrolyte concentrations, TBBA disturbed the assembly of the system. This difference may be explained by the fact that inclusion of TBBA inside the cyclodextrin cavities may decrease the hydrophilic character of polyCTR-βCD, as a consequence, interactions with the next chitosan layer would be decreased, and thereby the build-up of the whole assembly would be affected.

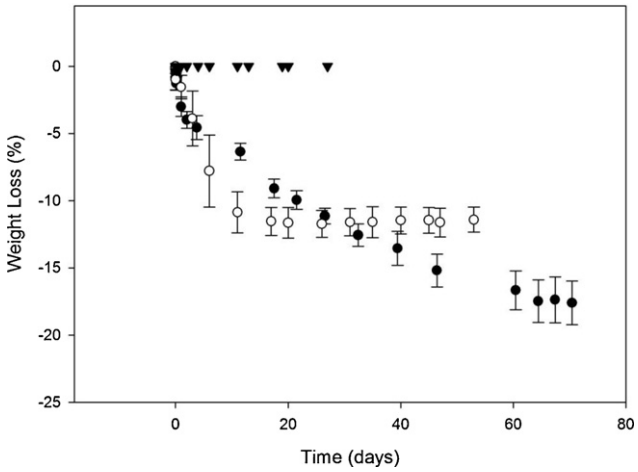


**Fig. 13.** Degradation of treated samples as a function of their weight loss against time in distilled water at 37 °C; (▼) virgin PET; (●) 20 layers, [chitosan] = 5 g/L in 10 mL/L HAc and [polyCTR-βCD] = 4 g/L in $H_2O$; (○) 20 layers + TBBA, [chitosan] = 5 g/L in 10 mL/L HAc and [polyCTR-βCD] = 4 g/L + 50 mg/L TBBA in $H_2O$.

#### 3.3.3. Stability of the multilayer assembly

The stability of the multilayer coating was followed by evolution of the sample weight immersed in water batches under stirring at 37 °C against time (Fig. 13).

The degradation of the samples that only underwent a pre-treatment step occurred within the 15 first days, corresponding to 12 wt% of the initial weight of the samples. This result displayed the degradation of the thermofixed layer through the esterolysis of the crosslinks. We can note that this degradation was not complete as the initial WG of the sample after pre-treatment was 19.6 wt%.

Besides, the extent of the weight loss of samples modified with 20 layers reached 17.8 wt% within 70 days. This degradation was slower than that observed on the only pre-treated sample,

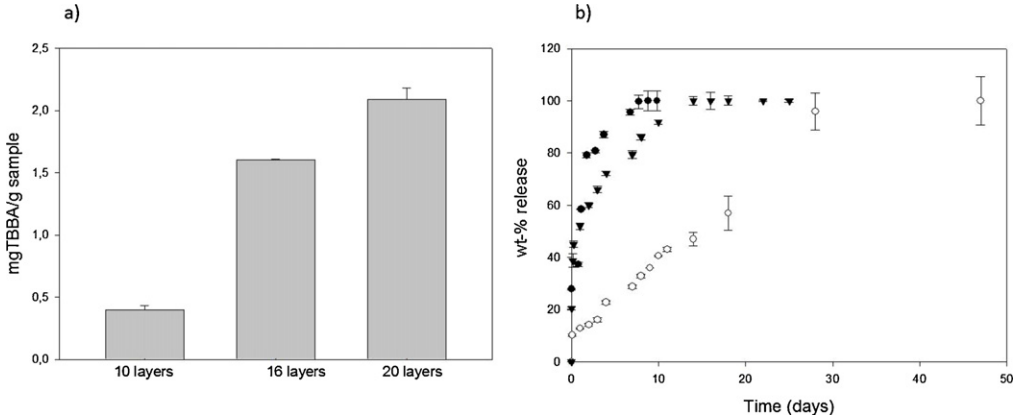


**Fig. 14.** (a) TBBA in mg per gram of sample adsorbed and released from samples treated with 10, 16 and 20 layers in water at 37 °C under stirring; (b) release kinetic study of TBBA from treated samples; (●) 10 layers; (▼) 16 layers; (○) 20 layers expressed in percentage with regard to data from (a).

indicating the relative stabilization of the assembly by the chitosan layers in the coating. As the initial WG of this series was 47 wt% after functionalization, it can be deduced that this value decreased down to 29 wt% after 70 days. Concerning TBBA loaded samples coated with 20 layers, a weight loss was clearly observed within the first 10 days (10.9%), and then continued with a slower rate indicating the potentiality of such system to operate as drug delivery system. In this context, the kinetics of release of TBBA was assessed in order to evaluate the drug-delivery properties of those new systems.

### 3.3.4. Release studies

A release study of TBBA from samples treated with 10, 16 and 20 layers was assessed in water at 37 °C. The maximal loading capacity of these three series of samples was calculated from the plateau values of each experiment and reported in Fig. 14a. Though TBBA preliminarily loaded onto the samples increased with the number of layers, the evolution did not obey to a strict proportionality rule. This result was due to the fact that increased amounts of both polyelectrolytes were adsorbed on the surface as the number of layers increased within the investigated range, as observed in the OWLS study.

Fig. 14b indicates that all immobilized TBBA onto treated textile samples was released within 7, 14 and 27 days for samples treated with 10, 16 and 20 layers, respectively. These results indicate that the release kinetics of TBBA could be controlled by the number of layers. As no direct correlation was observed with the degradation kinetics study mentioned above, it can be deduced that TBBA release was controlled by diffusion phenomena through the multilayer assembly rather than by the erosion of the multilayer system.

## 4. Conclusion

In this paper, we showed the possibility to build a drug delivery system based on the coating of multilayer incorporating a β-cyclodextrin polymer and chitosan, as negative and positive polyelectrolytes respectively. After monitoring this binary system by using the OWLS technique, it was applied to a PET non-woven textile after a pre-treatment aiming to give an ionic character to the latter, allowing the further deposition of the multilayer coating. Up to 20 layers could be superimposed, with or without TBBA as model bioactive model molecule in the system. A lesser amount of both polyelectrolytes were fixed on the support in presence of TBBA, due to a change in the hydrophilicity of the cyclodextrin polymer containing layers. It was observed that TBBA loading and its release time were both directly linked to the number of self-assembled layers present in the systems. As the degradation of the multilayer assembly in water batches occurred with a different kinetic, it was deduced that TBBA was released by diffusion process through the multilayer coating indicating the potentiality of such systems to operate in drug delivery applications. After this preliminary study, the use of a higher molecular weight chitosan and the influence of a crosslinking reaction step will be investigated in order to better control both the degradation of the multilayer coating and the diffusion of the model drug inside this structure. Our ultimate goal will be to extend this concept to the functionalization of more well defined medical devices incorporating drugs, like antibiotics or antiseptic agents. These results will be published in due course.

## Acknowledgements

Thanks to the University of Lille 1 who supported this work by awarding a PhD grant to the first author of this paper. The zeta potential measurements were developed by Mr. L. Royer in the frame of his end course of engineering studies cursus, supervised by Prof. Christine Campagne in the premises of Ecole Nationale Supérieure des Arts et Industries Textiles (ENSAIT), Roubaix, France.

## References

Abdelkebir, K., Gaudiere, F., Morin-Grognet, S., Coquerel, G., Labat, B., Atmani, H., et al. (2011). Evidence of different growth regimes coexisting within biomimetic layer-by-layer films. *Soft Matter*, *7*(19), 9197–9205.

Auzély-Velty, R., & Rinaudo, M. (2001). Chitosan derivatives bearing pendant cyclodextrin cavities: Synthesis and inclusion performance. *Macromolecules*, *34*(11), 3574–3580.

Bakkour, Y., Vermeersch, G., Morcellet, M., Boschin, F., Martel, B., & Azaroual, N. (2006). Formation of cyclodextrin inclusion complexes with doxycyclin-hyclate: NMR investigation of their characterisation and stability. *Journal of Inclusion Phenomena and Macrocyclic Chemistry*, *54*(1), 109–114.

Benkirane-Jessel, N., Schwinté, P., Falvey, P., Darcy, R., Haïkel, Y., Schaaf, P., et al. (2004). Build-up of polypeptide multilayer coatings with anti-inflammatory properties based on the embedding of piroxicam-cyclodextrin complexes. *Advanced Functional Materials*, *14*(2), 174–182.

Bhardwaj, N., & Kundu, S. C. (2011). Silk fibroin protein and chitosan polyelectrolyte complex porous scaffolds for tissue engineering applications. *Carbohydrate Polymers*, *85*(2), 325–333.

Blanchemain, N., Haulon, S., Martel, B., Traisnel, M., Morcellet, M., & Hildebrand, H. F. (2005). Vascular PET prostheses surface modification with cyclodextrin coating: Development of a new drug delivery system. *European Journal of Vascular and Endovascular Surgery*, *29*(6), 628–632.

Blanchemain, N., Haulon, S., Boschin, F., Marcon-Bachari, E., Traisnel, M., Morcellet, M., et al. (2007). Vascular prostheses with controlled release of antibiotics: Part 1. Surface modification with cyclodextrins of PET prostheses. *Biomolecular Engineering*, *24*(1), 149–153.

Blanchemain, N., Laurent, T., Haulon, S., Traisnel, M., Neut, C., Kirkpatrick, J., et al. (2007). In vitro study of a HPγ-cyclodextrin grafted PET vascular prosthesis for application as anti-infectious drug delivery system. *Journal of Inclusion Phenomena and Macrocyclic Chemistry*, *57*(1), 675–681.

Blanchemain, N., Karrout, Y., Tabary, N., Neut, C., Bria, M., Siepmann, J., et al. (2011). Methyl-β-cyclodextrin modified vascular prosthesis: Influence of the modification level on the drug delivery properties in different media. *Acta Biomaterialia*, *7*(1), 304–314.

Boschin, F., Blanchemain, N., Bria, M., Delcourt-Debruyne, E., Morcellet, M., Hildebrand, H. F., et al. (2006). Improved drug delivery properties of PVDF membranes functionalized with β-cyclodextrin—Application to guided tissue regeneration in periodontology. *Journal of Biomedical Materials Research: Part A*, *79A*(1), 78–85.

Brusatori, M. A., & Van Tassel, P. R. (2003). *Biosensing under an applied voltage using optical waveguide lightmode spectroscopy*. Kidlington: ROYAUME-UNI, Elsevier.

Burke, S. E., & Barrett, C. J. (2003). pH-responsive properties of multilayered poly(L-lysine)/hyaluronic acid surfaces. *Biomacromolecules*, *4*(6), 1773–1783.

Caruso, F., Niikura, K., Furlong, D. N., & Okahata, Y. (1997). Assembly of alternating polyelectrolyte and protein multilayer films for imiminosensing. *Langmuir*, *13*(13), 3427–3433.

Chen, W., & McCarthy, T. J. (1997). Layer-by-layer deposition: A tool for polymer surface modification. *Macromolecules*, *30*(1), 78–86.

Connors, K. A. (1997). The stability of cyclodextrin complexes in solution. *Chemical Reviews (Washington, DC, United States)*, *97*(5), 1325–1358.

Costa-Júnior, E. S., Barbosa-Stancioli, E. F., Mansur, A. A. P., Vasconcelos, W. L., & Mansur, H. S. (2009). Preparation and characterization of chitosan/poly(vinyl alcohol) chemically crosslinked blends for biomedical applications. *Carbohydrate Polymers*, *76*(3), 472–481.

Decher, G. (1997). Fuzzy nanoassemblies: Toward layered polymeric multicomposites. *Science*, *277*(5330), 1232–1237.

Decher, G., Hong, J. D., & Schmitt, J. (1992). Buildup of ultrathin multilayer films by a self-assembly process: III. Consecutively alternating adsorption of anionic and cationic polyelectrolytes on charged surfaces. *Thin Solid Films*, *210–211, Part 2*(0), 831–835.

Decher, G., & Schmitt, J. (1992). Fine-tuning of the film thickness of ultrathin multilayer films composed of consecutively alternating layers of anionic and cationic polyelectrolytes. *Trends in Colloid and Interface Science VI*, *89*, 160–164.

Degoutin, S., Jimenez, M., Casetta, M., Bellayer, S., Chai, F., Blanchemain, N., et al. (2012). Anticoagulant and antimicrobial finishing of non-woven polypropylene textiles. *Biomedical Materials*, *7*(3).

Deng, H., Zhou, X., Wang, X., Zhang, C., Ding, B., Zhang, Q., et al. (2010). Layer-by-layer structured polysaccharides film-coated cellulose nanofibrous mats for cell culture. *Carbohydrate Polymers*, *80*(2), 475–480.

Dubacheva, G. V., Dumy, P., Auzely, R., Schaaf, P., Boulmedais, F., Jierry, L., et al. (2010). Unlimited growth of host–guest multilayer films based on functionalized neutral polymers. *Soft Matter*, *6*(16), 3747–3750.

Dubas, S. T., & Schlenoff, J. B. (2001). Polyelectrolyte multilayers containing a weak polyacid: Construction and deconstruction. *Macromolecules*, *34*(11), 3736–3740.

Ducoroy, L., Bacquet, M., Martel, B., & Morcellet, M. (2007). Ion exchange textiles from the finishing of PET fabrics with cyclodextrins and citric acid for the sorption of metallic cations in water. *Journal of Inclusion Phenomena and Macrocyclic Chemistry*, *57*(1–4), 271–277.

Ducoroy, L., Martel, B., Bacquet, M., & Morcellet, M. (2007). Cation exchange finishing of nonwoven polyester with polycarboxylic acids and cyclodextrins. *Journal of Applied Polymer Science*, *103*(6), 3730–3738.

Ducoroy, L., Bacquet, M., Martel, B., & Morcellet, M. (2008). Removal of heavy metals from aqueous media by cation exchange nonwoven PET coated with β-cyclodextrin-polycarboxylic moieties. *Reactive and Functional Polymers*, *68*(2), 594–600.

Eggleston, C. M., Vörös, J., Shi, L., Lower, B. H., Droubay, T. C., & Colberg, P. J. S. (2008). Binding and direct electrochemistry of OmcA, an outer-membrane cytochrome from an iron reducing bacterium, with oxide electrodes: A candidate biofuel cell system. *Inorganica Chimica Acta*, *361*(3), 769–777.

El Ghoul, Y., Blanchemain, N., Laurent, T., Campagne, C., El Achari, A., Roudesli, S., et al. (2008). Chemical, biological and microbiological evaluation of cyclodextrin finished polyamide inguinal meshes. *Acta Biomaterialia*, *4*(5), 1392–1400.

Elvin, C. M., Vuocolo, T., Brownlee, A. G., Sando, L., Huson, M. G., Liyou, N. E., et al. (2010). A highly elastic tissue sealant based on photopolymerised gelatin. *Biomaterials*, *31*(32), 8323–8331.

Franklin, J. E., Marler, J. J., Byrne, M. T., Melvin, A. J., Clarson, S. J., & Melvin, D. B. (2009). Fiber technology for reliable repair of skeletal muscle. *Journal of Biomedical Materials Research – Part B: Applied Biomaterials*, *90B*(1), 259–266.

Franz, S., Rammelt, S., Scharnweber, D., & Simon, J. C. (2011). Immune responses to implants – A review of the implications for the design of immunomodulatory biomaterials. *Biomaterials*, *32*(28), 6692–6709.

Fu, J., Ji, J., Yuan, W., & Shen, J. (2005). Construction of anti-adhesive and antibacterial multilayer films via layer-by-layer assembly of heparin and chitosan. *Biomaterials*, *26*(33), 6684–6692.

García-González, C. A., Alnaief, M., & Smirnova, I. (2011). Polysaccharide-based aerogels – Promising biodegradable carriers for drug delivery systems. *Carbohydrate Polymers*, *86*(4), 1425–1438.

Gendron, R., Kumar, M. R., Paradis, H., Martin, D., Ho, N., Gardiner, D., et al. (2012). Controlled cell proliferation on an electrochemically engineered collagen scaffold. *Macromolecular Bioscience*, *12*(3), 360–366.

Gray, J. J. (2004). The interaction of proteins with solid surfaces. *Current Opinion in Structural Biology*, *14*(1), 110–115.

Gribova, V., Auzely-Velty, R., & Picart, C. (2011). Polyelectrolyte multilayer assemblies on materials surfaces: From cell adhesion to tissue engineering. *Chemistry of Materials*, *24*(5), 854–869.

Hamerli, P., Weigel, T., Groth, T., & Paul, D. (2003). Surface properties of and cell adhesion onto allylamine-plasma-coated polyethylenterephtalat membranes. *Biomaterials*, *24*(22), 3989–3999.

Jang, Y., Akgun, B., Kim, H., Satija, S., & Char, K. (2012). Controlled release from model blend multilayer films containing mixtures of strong and weak polyelectrolytes. *Macromolecules*, *45*(8), 3542–3549.

Joudieh, S., Bon, P., Martel, B., Skiba, M., & Lahiani-Skiba, M. (2009). Cyclodextrin polymers as efficient solubilizers of albendazole: Complexation and physicochemical characterization. *Journal of Nanoscience and Nanotechnology*, *9*(1), 132–140.

Karimpil, J. J., Melo, J. S., & D'Souza, S. F. (2012). Immobilization of lipase on cotton cloth using the layer-by-layer self-assembly technique. *International Journal of Biological Macromolecules*, *50*(1), 300–302.

Köstler, S., Ribitsch, V., Stana-Kleinschek, K., Jakopic, G., & Strnad, S. (2005). Electrokinetic investigation of polyelectrolyte adsorption and multilayer formation on a polymer surface. *Colloids and Surfaces A: Physicochemical and Engineering Aspects*, *270–271*(1–3), 107–114.

Kurrat, R., Textor, M., Ramsden, J. J., Boni, P., & Spencer, D. N. (1997). Instrumental improvements in optical waveguide light mode spectroscopy for the study of biomolecule adsorption. *Review of Scientific Instruments*, *68*(5), 2172–2176.

Kurrat, R., Prenosil, J. E., & Ramsden, J. J. (1997). Kinetics of human and bovine serum albumin adsorption at silica–titania surfaces. *Journal of Colloid and Interface Science*, *185*(1), 1–8.

Laurent, T., Kacem, I., Blanchemain, N., Cazaux, F., Neut, C., Hildebrand, H. F., et al. (2011). Cyclodextrin and maltodextrin finishing of a polypropylene abdominal wall implant for the prolonged delivery of ciprofloxacin. *Acta Biomaterialia*, *7*(8), 3141–3149.

Lavalle, P., Gergely, C., Cuisinier, F. J. G., Decher, G., Schaaf, P., Voegel, J. C., et al. (2002). *Comparison of the structure of polyelectrolyte multilayer films exhibiting a linear and an exponential growth regime: An in situ atomic force microscopy study*. Washington, DC: ETATS-UNIS, American Chemical Society.

Lawrence, N. J., Wells-Kingsbury, J. M., Ihrig, M. M., Fangman, T. E., Namavar, F., & Cheung, C. L. (2012). Controlling *E. coli* adhesion on high-k dielectric bioceramics films using poly(amino acid) multilayers. *Langmuir*, *28*(9), 4301–4308.

Lee, D. W., Lim, H., Chong, H. N., & Shim, W. S. (2009). Advances in chitosan material and its hybrid derivatives: A review. *Open Biomaterials Journal*, *1*, 10–20.

Leprêtre, S., Boschin, F., Tabary, N., Bria, M., Martel, B., Blanchemain, N., et al. (2007). Guided tissue regeneration membranes with controlled delivery properties of chlorhexidine by their functionalization with cyclodextrins. *Journal of Inclusion Phenomena and Macrocyclic Chemistry*, *57*(1), 297–302.

Leprêtre, S., Chai, F., Hornez, J. C., Vermet, G., Neut, C., Descamps, M., et al. (2009). Prolonged local antibiotics delivery from hydroxyapatite functionalised with cyclodextrin polymers. *Biomaterials*, *30*(30), 6086–6093.

Li, J., Xiao, H., Li, J., & Zhong, Y. (2004). Drug carrier systems based on water-soluble cationic [beta]-cyclodextrin polymers. *International Journal of Pharmaceutics*, *278*(2), 329–342.

Lin, Q. K., Ren, K. F., & Ji, J. (2009). Hyaluronic acid, chitosan-DNA complex multilayered thin film as surface-mediated nonviral gene delivery system. *Colloids, Surfaces B: Biointerfaces*, *74*(1), 298–303.

Loftsson, T., & Brewster, M. E. (1996). Pharmaceutical applications of cyclodextrins: 1. Drug solubilization and stabilization. *Journal of Pharmaceutical Sciences*, *85*(10), 1017–1025.

Lvov, Y., Decher, G., & Moehwald, H. (1993). Assembly, structural characterization, and thermal behavior of layer-by-layer deposited ultrathin films of poly(vinyl sulfate) and poly(allylamine). *Langmuir*, *9*(2), 481–486.

Lvov, Y., Ariga, K., Ichinose, I., & Kunitake, T. (1995). Assembly of multicomponent protein films by means of electrostatic layer-by-layer adsorption. *Journal of the American Chemical Society*, *117*(22), 6117–6123.

Martel, B., Morcellet, M., Ruffin, D., Ducoroy, L., & Weltrowski, M. (2002). Finishing of polyester fabrics with cyclodextrins and polycarboxylic acids as crosslinking agents. *Journal of Inclusion Phenomena*, *44*(1–4), 443–446.

Martel, B., Morcellet, M., & Weltrowski, M. (2002). Cyclodextrin polymers and/or cyclodextrin derivatives with complexing properties and ion exchange. Properties and method for the production thereof US 6,660,804 B1, 2003.

Martel, B., Weltrowski, M., Ruffin, D., & Morcellet, M. (2002). Polycarboxylic acids as crosslinking agents for grafting cyclodextrins onto cotton and wool fabrics: Study of the process parameters. *Journal of Applied Polymer Science*, *83*(7), 1449–1456.

Martel, B., Ruffin, D., Weltrowski, M., Lekchiri, Y., & Morcellet, M. (2005). Water-soluble polymers and gels from the polycondensation between cyclodextrins and poly(carboxylic acid)s: A study of the preparation parameters. *Journal of Applied Polymer Science*, *97*(2), 433–442.

Ngankam, A. P., Mao, G., & Van Tassel, P. R. (2004). Fibronectin adsorption onto polyelectrolyte multilayer films. *Langmuir*, *20*(8), 3362–3370.

Ngankam, A. P., & Van Tassel, P. R. (2005). In situ layer-by-layer film formation kinetics under an applied voltage measured by optical waveguide lightmode spectroscopy. *Langmuir*, *21*(13), 5865–5871.

Nițescu, M., Dumitriu, A. S., Dumitru, S. G., Trăistaru, M., & Burlibaşa, M. (2012). Surface treatment methods for titanium implants. *Metalurgia International*, *17*(6), 147–150.

Pedroni, V. I., Gschaider, M. E., & Schulz, P. C. (2003). UV spectrophotometry: Improvements in the study of the degree of acetylation of chitosan. *Macromolecular Bioscience*, *3*(10), 531–534.

Picart, C., Ladam, G., Senger, B., Voegel, J. C., Schaaf, P., Cuisinier, F. J. G., et al. (2001). Determination of structural parameters characterizing thin films by optical methods: A comparison between scanning angle reflectometry and optical waveguide lightmode spectroscopy. *Journal of Chemical Physics*, *115*(2), 1086–1094.

Rajewski, R. A., & Stella, V. J. (1996). Pharmaceutical applications of cyclodextrins: 2. In vivo drug delivery. *Journal of Pharmaceutical Sciences*, *85*(11), 1142–1169.

Rinaudo, M. (2006). Chitin and chitosan: Properties and applications. *Progress in Polymer Science (Oxford)*, *31*(7), 603–632.

Scott, E. A., Nichols, M. D., Cordova, L. H., George, B. J., Jun, Y.-S., & Elbert, D. L. (2008). Protein adsorption and cell adhesion on nanoscale bioactive coatings formed from poly(ethylene glycol) and albumin microgels. *Biomaterials*, *29*(34), 4481–4493.

Seantier, B. A., & Deratani, A. (2012). *Ionic interactions in natural and synthetic macromolecules*. Hoboken, NJ: John Wiley & Sons, Inc.

Semenov, A., Charlot, A., Auzély-Velty, R., & Rinaudo, M. (2007). Rheological properties of binary associating polymers. *Rheologica Acta*, *46*(5), 541–568.

Smole, M., Stana-Kleinschek, K., Ribitsch, V., Pointner, B., Zipper, P., Stakne, K., et al. (2002). Electrokinetic properties of surface modified PETP fibres. *Materials Research Innovations*, *6*(1), 19–23.

Sun, T., Guo, Q., Zhang, C., Hao, J., Xing, P., Su, J., et al. (2012). Self-assembled vesicles prepared from amphiphilic cyclodextrins as drug carriers. *Langmuir*, *28*(23), 8625–8636.

Tabary, N., Lepretre, S., Boschin, F., Blanchemain, N., Neut, C., Delcourt-Debruyne, E., et al. (2007). Functionalization of PVDF membranes with carbohydrate derivates for the controlled delivery of chlorhexidin. *Biomolecular Engineering*, *24*(5), 472–476.

Tang, W., Zhao, J., Sha, B., & Liu, H. (2012). Adsorption and drug release based on β-cyclodextrin-grafted hydroxyapatite composite. *Journal of Applied Polymer Science*, *127*(4), 2803–2808.

Teo, E. Y., Ong, S. Y., Khoon Chong, M. S., Zhang, Z., Lu, J., Moochhala, S., et al. (2011). Polycaprolactone-based fused deposition modeled mesh for delivery of antibacterial agents to infected wounds. *Biomaterials*, *32*(1), 279–287.

Tie, Y., Calonder, C., & Van Tassel, P. R. (2003). Protein adsorption: Kinetics and history dependence. *Journal of Colloid and Interface Science*, *268*(1), 1–11.

Tiefenthaler, K., & Lukosz, W. (1989). *Sensitivity of grating couplers as integrated-optical chemical sensors*. Washington, DC: ETATS-UNIS, Optical Society of America.

Uchida, E., Uyama, Y., & Ikada, Y. (1993). Sorption of low-molecular-weight anions into thin polycation layers grafted onto a film. *Langmuir*, *9*(4), 1121–1124.

Uekama, K., Hirayama, F., & Irie, T. (1998). Cyclodextrin drug carrier systems. *Chemical Reviews (Washington, DC, United States)*, *98*(5), 2045–2076.

Venkatesan, J., Ryu, B., Sudha, P. N., & Kim, S. K. (2012). Preparation and characterization of chitosan-carbon nanotube scaffolds for bone tissue engineering. *International Journal of Biological Macromolecules*, *50*(2), 393–402.

Vörös, J., Ramsden, J. J., Csúcs, G., Szendrő, I., De Paul, S. M., Textor, M., et al. (2002). Optical grating coupler biosensors. *Biomaterials*, *23*(17), 3699–3710.

Wang, Q., & Hauser, P. (2009). New characterization of layer-by-layer self-assembly deposition of polyelectrolytes on cotton fabric. *Cellulose*, *16*(6), 1123–1131.

Weickenmeier, M., Wenz, G., & Huff, J. (1997). Association thickener by host guest interaction of a β-cyclodextrin polymer and a polymer with hydrophobic side-groups. *Macromolecular Rapid Communications*, *18*(12), 1117–1123.

Weisser, M., Nelles, G., Wenz, G., & Mittler-Neher, S. (1997). Guest–host interactions with immobilized cyclodextrins. *Sensors and Actuators B: Chemical*, *38*(1–3), 58–67.

Wenz, G., Strassnig, C., Thiele, C., Engelke, A., Morgenstern, B., & Hegetschweiler, K. (2008). Recognition of ionic guests by ionic β-cyclodextrin derivatives. *Chemistry: A European Journal*, *14*(24), 7202–7211.

Wittmer, C. R., Phelps, J. A., Saltzman, W. M., & Van Tassel, P. R. (2007). Fibronectin terminated multilayer films: Protein adsorption and cell attachment studies. *Biomaterials*, *28*(5), 851–860.

Wyrzykowski, D., Hebanowska, E., Nowak-Wiczk, G., Makowski, M., & Chmurzyński, L. (2011). Thermal behaviour of citric acid and isomeric aconitic acids. *Journal of Thermal Analysis and Calorimetry*, *104*(2), 731–735.